

RESEARCH

Open Access



Post-stroke Stiff-Knee gait: are there different types or different severity levels?

Jeonghwan Lee¹, Bryant A. Seamon², Robert K. Lee³, Steven A. Kautz⁴, Richard R. Neptune¹ and James S. Sulzer^{5,6*}

Abstract

Stiff-Knee gait (SKG) commonly occurs in individuals after stroke, loosely defined as reduced peak knee flexion angle during swing. The causes of SKG are multifaceted and debated. Further, clinical interventions have not been consistently effective, possibly resulting from multiple undiagnosed subtypes of SKG. Thus, our primary goal of this study is to explore the existence of potential subtypes associated with different levels of motor control complexity. We used retrospective kinematics, kinetics and muscle activity from 50 stroke survivors and 15 healthy, age-matched controls during treadmill walking. We used a time-series kernel k-means cluster analysis based on compensatory frontal plane kinematics associated with SKG to separate participants into three groups, Cluster A (hip hiking, lowest knee flexion, highest propulsion asymmetry, lowest gait speed), Cluster B (hip hiking and hip abduction, moderate knee flexion, middle gait speed) and Cluster C (highest knee flexion, highest gait speed). The highest proportion of individuals with SKG as diagnosed by a clinician were in Cluster A, but with a substantial proportion in Cluster B, indicating that these two clusters can be considered subtypes of SKG. Despite differences in kinematics and kinetics, we did not observe fundamental differences in underlying motor control between clusters as determined by non-negative matrix factorization of measured muscle activations. We conclude that the differences between clusters were most likely attributed to the severity of gait impairment, as reflected by slower gait speed and propulsion asymmetry, rather than being a different type of SKG.

Introduction

Reduced knee flexion during gait following neurological injury such as stroke is very common, with estimated prevalence between 25 and 75% of those with gait impairments [1, 2]. Such reduced or delayed knee flexion during the swing phase, which impairs effective ground clearance and forward progression, is defined as Stiff-Knee gait (SKG) [3]. Post-stroke SKG has been attributed to various causes, including weakness of hamstrings [4], hip flexors [5] and/or plantarflexors [1, 6], motor incoordination [7, 8] and, most commonly, hyperreflexia of the quadriceps [9]. The existence of different etiologies of SKG could help explain the inconsistent results observed from interventions, particularly chemodenervation of the spastic quadriceps [10, 11]. Thus, identifying subtypes of post-stroke SKG may help lead towards more appropriate treatments.

*Correspondence:
James S. Sulzer
jss280@case.edu

¹ Walker Department of Mechanical Engineering, University of Texas at Austin, 204 E Dean Keeton St, Austin, TX 78712, USA

² Department of Rehabilitation Sciences, College of Health Professions, The Medical University of South Carolina, 151 Rutledge Ave Building B, Charleston, SC 29425, USA

³ St. David's Medical Center, 3000 N Interstate Hwy 35 #660, Austin, TX 78705, USA

⁴ Department of Health Sciences and Research, College of Health Professions, The Medical University of South Carolina, 77 President Street, Charleston, SC 29425, USA

⁵ Department of Physical Medicine and Rehabilitation, The MetroHealth System, 2500 MetroHealth Drive, Cleveland, OH 44109, USA

⁶ Department of Physical Medicine and Rehabilitation, Case Western Reserve University, 10900 Euclid Ave, Cleveland, OH 44106, USA



© The Author(s) 2025. **Open Access** This article is licensed under a Creative Commons Attribution-NonCommercial-NoDerivatives 4.0 International License, which permits any non-commercial use, sharing, distribution and reproduction in any medium or format, as long as you give appropriate credit to the original author(s) and the source, provide a link to the Creative Commons licence, and indicate if you modified the licensed material. You do not have permission under this licence to share adapted material derived from this article or parts of it. The images or other third party material in this article are included in the article's Creative Commons licence, unless indicated otherwise in a credit line to the material. If material is not included in the article's Creative Commons licence and your intended use is not permitted by statutory regulation or exceeds the permitted use, you will need to obtain permission directly from the copyright holder. To view a copy of this licence, visit <http://creativecommons.org/licenses/by-nc-nd/4.0/>.

Post-stroke SKG may not be best explained solely by its most visible manifestation, reduced knee flexion, but rather by a complex interplay of multiple biomechanical gait parameters and underlying neural control deficits. While reduced knee flexion is the hallmark of SKG, earlier gait research in those with stroke and cerebral palsy highlighted the impaired initial swing phase characteristics, such as insufficient pre-swing knee flexion velocity, inadequate hip flexion, and persistent toe dragging [3, 12–14]. Compensatory strategies to address these impairments often involve distinct frontal plane movements, including hip abduction, hip hiking (pelvic obliquity), vaulting (contralateral foot rise) and pelvic lag (paretic pelvic external rotation during swing) [12, 15–17]. These compensatory actions vary across individuals, as some may be consciously controlled while others occur involuntarily due to more extensive neuromuscular deficits. For instance, evidence suggests that excessive hip abduction in post-stroke SKG may be linked to disrupted motor coordination patterns [18, 19]. Studies have highlighted that stroke survivors exhibit altered muscle modules, which contribute to impaired swing-phase knee flexion due to inappropriate muscle activation timing and merging of distinct muscle modules [20–23]. This merging is likely stems from abnormal reflex pathway, such as hyperexcitable reflex [24] and abnormal inter-joint coupling [25]. A recent study identified two distinct patterns in individuals with SKG compared to those without: synergy simplification and abnormal timing and activation, emphasizing the combined impact of neuromuscular deficits in SKG [26]. These findings suggest the potential existence of subtypes of SKG that stem from broader neuromuscular deficits rather than isolated joint-level dysfunctions, which could be differentiated by distinct compensatory movement patterns.

Due to the growing evidence of the link between muscle coordination patterns and SKG, our goal was to investigate whether distinct subtypes exist of those with reduced swing phase knee flexion angle after stroke. We examined gait data from 50 individuals post-stroke and 15 healthy, age-matched controls. Instead of categorizing these individuals by knee flexion angle, we categorized by frontal plane motions using time-series kernel k-means cluster analysis (i.e., we separated those post-stroke by the effects of SKG). We then compared the kinematics, kinetics, EMG and corresponding muscle coordination parameters of these groups. We hypothesized that (1) we would find multiple clusters of those with a high proportion of SKG as defined by a clinician signifying different subtypes, and (2) those subtypes would be differentiated by muscle coordination patterns. This work is a novel investigation into subtypes of post-stroke SKG, which can lead to a more precise definition, or multiple

definitions, of SKG that will better homogenize study populations and lead to personalized treatments.

Methods

Data source

Motion capture, force and electromyography (EMG) data were collected from 50 individuals post-stroke with hemiparesis (31 left hemiparesis, 31 males, 57.0 ± 13.5 years) and a control group of 15 healthy individuals (7 male, 54.5 ± 8.7 years) during walking. Participants provided informed written consent to the Institutional Review Board approved protocol. Participants walked on a split-belt instrumented treadmill (Bertec, Columbus, Ohio) at their self-selected speed. Of those, 43 individuals post-stroke also walked at their fastest possible speed. Prior to data collection, participants practiced treadmill walking to get comfortable with the experimental setup. Participants walked for at least 10 s to reach a steady-state walking pattern before each 30-s trial. Participants did not use an assistive device or orthotics during the data collection. Participants with severe ankle instability were allowed to use an ankle brace on the paretic side to prevent injury. The brace provided medial-lateral support but did not restrict ankle dorsi- and plantarflexion. Motion capture marker data were collected at 120 Hz using a 12-camera motion capture system (PhaseSpace, San Leandro, CA) with a modified Helen Hayes marker set using 65 active markers. EMG data were collected (Motion Labs, Cortlandt, NY) at 1000 Hz from bilateral electrodes placed on the medial gastrocnemius (GAS), soleus (SOL), tibialis anterior (TA), vastus medialis (VA), lateral hamstrings (LH), medial hamstrings (MH), rectus femoris (RF), and gluteus medius (GM). EMG data were high-pass filtered at 40 Hz, demeaned, rectified and low-pass filtered at 4 Hz. For each muscle, the filtered signal was normalized to its mean value of EMG envelope during each trial to reduce inter-individual variability [27]. Ground reaction force (GRF) data were measured by an embedded force plate in a split-belt treadmill and low-pass filtered at 15 Hz. Joint kinematics, body kinematics, and joint kinetics were calculated with the kinematics and dynamics solver within OpenSim 4.3 [28]. All synchronized time-series biomechanical gait data were divided into strides by a paretic limb heel-strike event using vertical GRFs and expressed as a percentage of the cycle time. Eight strides per participant were randomly selected from 30-s treadmill walking trials for further analysis.

We employed clinical diagnosis by an expert clinician (RKL) on post-stroke SKG as our baseline labels. We generated 3D animations with four different camera view angles from the motion captured data using OpenSim software. The expert clinician then reviewed these anonymized animated videos to diagnose whether

subjects exhibited post-stroke SKG. Table 1 summarized participants' demographics, walking speed and diagnosis.

Multivariate cluster analysis

Gait features associated with compensatory strategies

In this multivariate clustering, we based our analysis on the parameters specifically associated with supposed frontal-plane compensatory strategies following stroke. As multivariate clustering inputs, we used paretic pelvic obliquity, paretic hip abduction, and non-paretic hip abduction, which are all major components of hip circumduction and upward pelvic hiking following stroke. The underlying philosophy of the multivariate clustering was to define SKG based on motions associated with SKG, but not using disability-specific characteristics, such as knee flexion to avoid a bias towards this parameter. Individuals may compensate to reduced knee flexion in different ways; our goal was to classify these individuals based on those differences.

Time series K-mean clustering

Most gait biomechanics studies analyze kinematic data by focusing on discrete events, such as joint angles at key gait phases, and extracting descriptive statistics like peak angles and range of motion. However, these traditional approaches rely on a priori feature selection, often discarding substantial kinematic data that may contain critical information about between-group differences [29]. Time-series analysis provides significant advantages over conventional methods by preserving the temporal dynamics of gait data, enabling the detection of subtle variations and patterns that might be overlooked when data is discretized [30]. To leverage these benefits, we implemented a time-series kernel k-means algorithm with a global alignment kernel for clustering. The kernel

k-means [31] is an extension of the standard k-means algorithm using a kernel function for a distance/similarity computation to overcome the limiting assumption of linearly separable clusters. The global alignment kernel [32] enables use in a time-series context, which accounts for holistic pattern changes in time-series signals. In this work, we used a publicly available Python package, *tslearn* [33], to implement the aforementioned time-series kernel k-means clustering with multivariate inputs.

The number of clusters to be tested from the sample population was determined using inertia and silhouette scores. The inertia score is a measure of cohesion defined by the sum of squared distance of samples to their closest cluster center. The silhouette score is calculated using the mean intra-cluster distance and the mean nearest-cluster distance taking both cohesion and separation into account [34]. A relatively low inertia and high silhouette score indicate good quality clustering. Through the elbow method [35] with these two measures, we determined the number of clusters that are supposed to be in the sample population.

Outcome measures

Output clusters were analyzed with respect to representative gait patterns in those with post-stroke SKG, including gait speed and peak swing phase knee flexion angle. Time-course joint kinematics and kinetics in the sagittal and frontal plane were examined simultaneously. We also analyzed propulsive asymmetry as a measure of paretic limb function [36]. Muscle coordination was quantified using (1) timing of individual muscle activation signals, (2) module number and composition, and (3) the Dynamic Motor Control Index (DMCI) [37].

Module number and composition are calculated from non-negative matrix factorization (NNMF) of filtered

Table 1 Summary of participants demographics, walking speed, and SKG labeled by a clinical expert

	Healthy	SKG	Non-SKG
Age	54.5±8.7	52.8±15.1	59.6±11.4
Height (cm)	161.9±7.2	166.2±9.2	163.1±10.5
Weight (kg)	86.8±12.3	86.4±15.3	95.4±20.6
Gender (Female/Male)	8/7	7/17	12/14
Paretic Side (Left/Right)	N/A	11/13	8/18
Overground Walking Speed (m/s)	N/A	0.61±0.27	0.89±0.29
Comfortable Walking Speed (m/s)	0.73±0.22	0.32±0.18	0.46±0.21
Fastest Comfortable Walking Speed (m/s)	1.44±0.28	0.54±0.30	0.73±0.34
6-Minute Walk Test (m)	N/A	276.8±142.7	342.5±111.2
Fugl-Meyer Assessment	N/A	20.6±5.7	25.2±5.0
Dynamic Gait Index	N/A	15.9±3.2	17.3±3.7
Berg Balance Scale	N/A	47.4±4.9	50.5±4.8

EMG data from all 8 muscles on the paretic leg as previously described [7]. NNMF computes muscle weights (W) and their corresponding time-varying activations (H). This process was repeated through iterative optimization, starting with random initial estimates of W and H , and selecting the matrices that minimized the sum of squared errors between the activations predicted by $W \times H$ and the EMG data. NNMF also identified the minimum number of muscle modules required to explain more than 90% of the EMG variability, along with the weighted contribution of each muscle to each module. The variance in EMG data accounted for (VAF) by n modules is calculated as one minus the ratio of the sum of squared errors (SSE) and the total sum of squares of the EMG data (SST) calculated across the 101 points of the gait cycle, denoted as:

$$VAF = 1 - \frac{SSE}{SST} = \frac{\|EMG - W \times H\|^2}{\|EMG\|^2}. \quad (1)$$

We used DMCI in walking as a quantitative measure of motor control complexity. For instance, high DMCI represents a better motor control, coordination, and stability. It was derived using NNMF, with the total number of allowable muscle modules constrained to one. By limiting the number of modules to one, it minimized the influence of pre-processing techniques and cutoff criteria, which can yield inconsistent results in the number of identified muscle modules. Consequently, the DMCI holds significant potential as a robust summary metric for evaluating muscle co-activation patterns during walking [38]. DMCI is defined as:

$$DMCI = 100 + 10 \left(\frac{avgVAF_1^{Ctl} - VAF_1^{Exp}}{stdVAF_1^{Ctl}} \right) \quad (2)$$

where VAF_1^{Exp} represents the VAF of the one-synergy solution for each individual in the experimental groups (i.e., clustered post-stroke groups in this study), and $avgVAF_1^{Ctl}$ and $stdVAF_1^{Ctl}$ denote the average and standard deviation of the VAF for one-synergy solution of the healthy control group, respectively.

We examined the types of merged coordination patterns using module composition or the W matrix from the NNMF solution for each participant with 3 modules within clusters. These patterns were identified by correlating the muscle module weightings (i.e., W matrix) of each participant with those of unimpaired individuals, based on previously reported modules in unimpaired adults [7, 8, 23]. We also examined changes in module composition by comparing module weightings (W matrix) and timing curves (H matrix) from a 4-module fixed solution.

Statistics

We employed statistical parametric mapping (SPM) analysis to examine differences between clusters of one-dimensional time-series data. SPM can perform linear statistical testing (i.e., t-test, ANOVA, etc.) for time-series signals. Because SPM does not require assumptions and abstraction of signals dependent on the spatiotemporal foci of signals, it provides apparent and intuitive statistical results described in the original sampling space [30]. In this study, we performed SPM one-way ANOVA to compare clustered post-stroke gait patterns. As a part of post hoc analysis, we applied a pairwise two-tailed t-test with Bonferroni correction using SPM. SPM one-way ANOVA and its post hoc analyses were completed by an open source SPM1D package (<http://www.spm1d.org/>) [39] using Python version of 3.8.10.

To examine relationships and interactions of other discrete outcome measures (e.g., gait speed, propulsive asymmetry, number of motor modules) according to clusters, we used a linear mixed model and post hoc analysis using pairwise t-test with Bonferroni correction. A linear mixed model and multiple comparisons were done by *Statsmodels* package in Python [40].

Results

Outcomes suggested that 3 clusters were the best representation of the sample given the feature set. Figure 1 represents inertial and silhouette measures across a varying number of clusters to determine an optimal number of multivariate clusters. At 3 clusters, the inertia measure showed a relatively low decrease rate to the next number while the silhouette score was the highest. As a result, a total of 50 post-stroke individuals were separated into three clusters denoted as A ($n=14$), B ($n=23$), and C ($n=13$). Based on the baseline label by clinical expert, 10 individuals in Cluster A, 10 individuals in Cluster B, and 4 individuals in Cluster C were diagnosed as a post-stroke SKG.

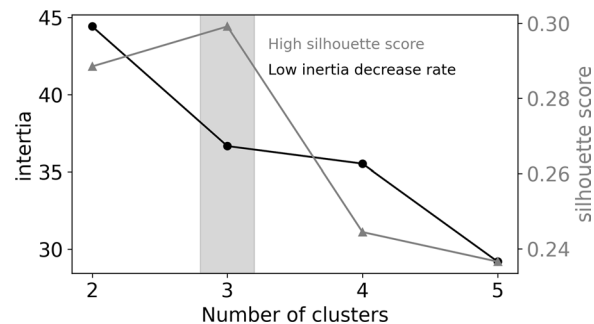


Fig. 1 Inertia and silhouette score changes for varying numbers of clusters. Lower inertia and high silhouette score indicate better quality of clusters

Gait speed and the peak knee flexion angle

Comparing between clusters and healthy controls, with the random intercept and slope model using a linear mixed model, we found significant differences in self-selected walking speed ($\beta=0.16$, $t=6.83$, $p<0.001$). Similarly, the peak swing-phase knee flexion angle exhibited significant group differences ($\beta=11.05$, $t=7.83$, $p<0.001$). Figure 2 visualizes post hoc test results between pairs for these outcomes. We observed incrementally increased walking speed and knee flexion angle with each cluster group and controls (i.e., A lowest, healthy controls highest). However, we did not find a statistically significant difference between Cluster B and C in either outcome measure ($p>0.05$).

Compensatory parameters

Commonly known compensatory motions following stroke, such as hip hiking, hip circumduction, and contralateral ankle vaulting were examined based on four kinematic profiles (i.e., paretic pelvic obliquity, paretic hip abduction, non-paretic hip abduction, and non-paretic ankle plantarflexion) by using SPM one-way ANOVA (Fig. 3) and post hoc multiple comparisons (Table 2). We observed statistically discernible patterns of pelvic motions (45.05–98.19% gait cycle, $F^*=5.316$, $p<0.001$), paretic hip abduction motions (70.57–83.25% gait cycle, $F^*=5.407$, $p<0.05$), and non-paretic hip abduction motions (40.414–93.54% gait cycle, $F^*=5.439$, $p<0.001$). There were no significant differences in non-paretic ankle motion. Note that F^* denotes a critical threshold for SPM one-way ANOVA, equivalent to F-statistic. Specifically, people in Cluster A had 6.74° more peak pelvic obliquity than Cluster B, 8.48° more than Cluster C, and 8.81° more than in healthy controls. Cluster A initiated hip hiking in

the pre-swing phase, but Cluster B initiated hip hiking in the swing phase. Cluster A had 6.94° less peak hip abduction than healthy controls ($p<0.001$). Like pelvic obliquity, individuals in Cluster A exhibited 7.42° greater peak non-paretic hip abduction compared to Cluster B, 8.88° more than Cluster C, and 8.77° more than healthy controls. A summary of statistical comparisons between all groups is shown in Table 2.

Sagittal plane joint kinematics and kinetics differed between clusters. Figure 4 illustrates SPM one-way ANOVA results on the sagittal-plane joint kinematics and kinetics. We observed differences in pre-swing hip flexion angle (50.56–71.86% gait cycle, $F^*=4.970$, $p=0.032$), mid-stance hip moment (24.11–39.19% gait cycle, $F^*=6.690$, $p<0.001$), and pre-swing hip moment (44.45–60.59% gait cycle, $F^*=6.690$, $p<0.001$). Individuals in Cluster A had 18.65° less peak hip extension than Cluster B and 20.25° less than healthy controls in pre-swing. Cluster A had reduced peak hip extension moment, 28.60 Nm/kg less than Cluster B and 22.62 Nm/kg less than controls. People in Cluster A had 18.41° less peak knee flexion than Cluster C and 29.31° less peak knee flexion than controls. Cluster B had 22.12° less peak knee flexion than controls, but no significant difference between each other clusters. We observed differences in knee flexion moment (52.26–57.08% gait cycle, $F^*=6.825$, $p<0.05$), with individuals in Cluster B exhibiting 22.46 Nm/kg less than healthy controls. Ankle plantar flexion moment (44.83–63.56% gait cycle, $F^*=7.064$, $p<0.001$) showed differences, with individuals in Cluster A walking with 47.94 Nm/kg lower plantar flexion moment compared to healthy controls, and those in Cluster B with 36.08 Nm/kg less than controls. No significant differences in these parameters were observed

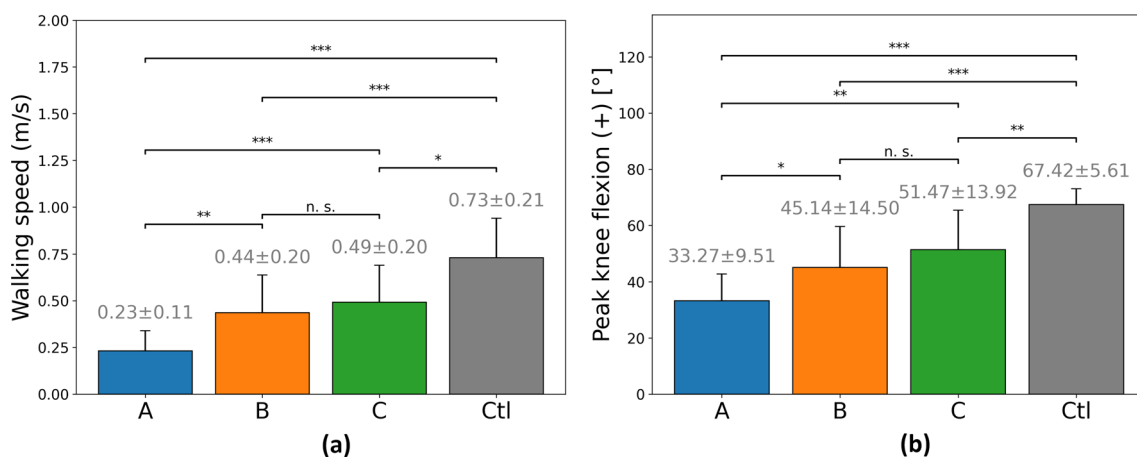


Fig. 2 Post hoc multiple comparisons for the self-selected gait speed (a) and the peak swing-phase knee flexion angle (b) across clusters by pairwise t-test with Bonferroni correction. Statistical significance denoted by *** ($p<0.001$), ** ($p<0.01$), * ($p<0.05$), and n.s. (not significant)

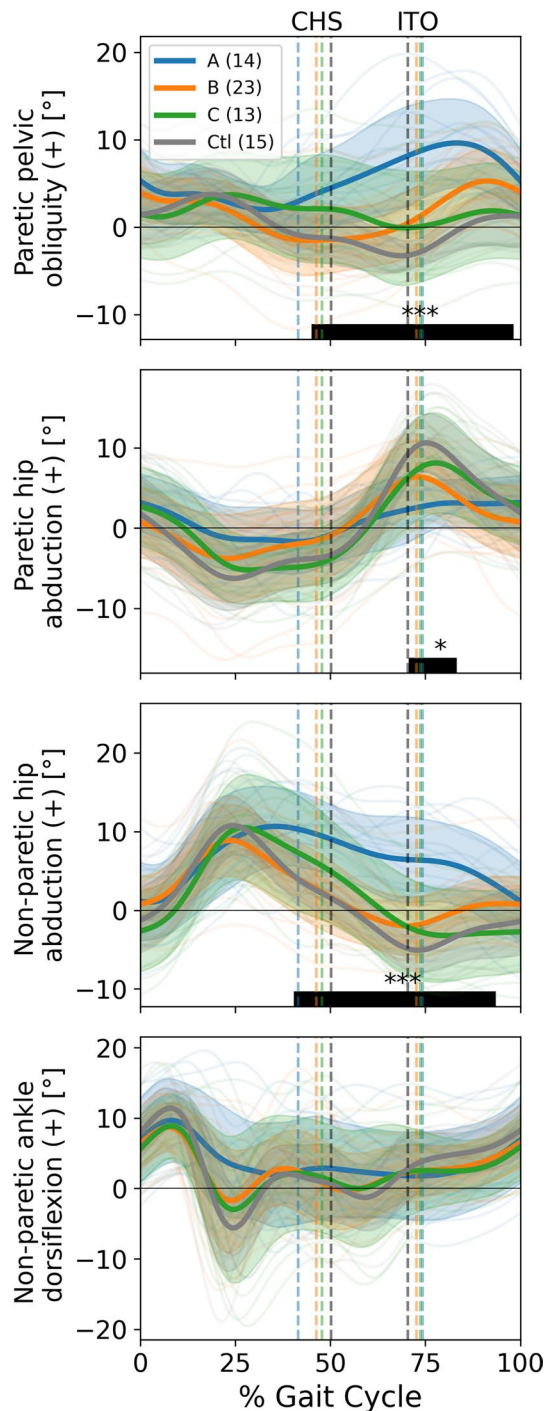


Fig. 3 Cluster-based SPM One-way ANOVA of compensatory motions. Solid black bars at the bottom show the statistically significant portion of the gait cycle as determined by SPM. Statistical significance denoted by *** ($p < 0.001$), ** ($p < 0.01$), and * ($p < 0.05$). The thick solid and shaded areas are average and standard deviations of each group, respectively. Thin solid lines in backgrounds represent individual data. Left and right vertical dashed lines indicate contralateral heel strike (CHS) and ipsilateral toe-off (ITO) events, respectively. The gait cycle is based on the paretic limb's heel strike (0%)

between people in Cluster C compared to people in Cluster B or healthy controls. Post hoc multiple comparisons are summarized in Tables 3 and 4.

Propulsive asymmetry

Using the random intercept and slope model of a linear mixed model, we found significant differences in the propulsive asymmetry ($\beta = -7.494$, $t = -5.267$, $p < 0.001$). Cluster A had significantly higher asymmetry compared to Clusters B, C, and healthy controls (Fig. 5). There were no significant propulsive asymmetry differences among Clusters B, C, and healthy controls.

Muscle activity

There were differences observed in muscle activity. Vastus medialis (24.74–41.09% gait cycle, $F^* = 6.728$, $p < 0.001$) and lateral hamstrings (11.27–40.10% gait cycle, $F^* = 6.737$, $p < 0.001$) showed differences between clusters during mid-stance (Fig. 6). Specifically, people in Cluster A and C had a greater vastus medialis activation than healthy controls. In lateral hamstrings, individuals in Cluster A had greater EMG activity than those in Cluster B, Cluster C and healthy controls. All other muscles' activation patterns were different from healthy controls, but there were no significant differences between clusters. Post hoc multiple comparisons for vastus medialis and lateral hamstrings muscle activation are summarized in Table 5.

Module analysis

We anticipated that clusters would differ in terms of muscle coordination. These coordination patterns, or muscle modules, can be revealed using non-negative matrix factorization of muscle activity [41]. Healthy individuals typically walk with four different modules. In comparison, the post-stroke individuals used between two and four modules, as shown in Fig. 7. Most post-stroke individuals in Cluster A had two or three modules (13 out of 14), with only one person exhibiting four modules. In contrast, most individuals in Cluster B had three or four modules (21 out of 23). Unlike other clusters, no individuals in Cluster C exhibited two modules.

We denoted the following merged patterns among individuals with three modules, the first type, where hip abductors, hip/knee extensors, and ankle plantar flexors muscle groups were merged, [8, 23] is denoted as 3M-MS1. The second type, where hip abductors, hip/knee extensors, and hamstrings muscle groups were merged [8, 23], is denoted as 3M-MS2. The third type, where hip flexors, ankle dorsiflexors, and knee flexors muscle groups were merged [23], is denoted as 3M-MS3. Any patterns that did not fit these categories were denoted as Not Classified (NC). The merged module

Table 2 Summary of between group post hoc comparisons based on compensatory motions

Comparison	Paretic Pelvic obliquity angle [°]	Paretic Hip Abd/Add Angle [°]	Non-paretic Hip Abd/Add Angle [°]
A-B	6.74 [3.61, 9.88]*** (44.03, 84.94)% gait cycle	–	7.42 [4.47, 10.38]*** (38.56, 85.68)% gait cycle
A-C	8.48 [4.04, 12.91]* (71.83, 90.16)% gait cycle	–	8.88 [4.48, 13.29]* (69.04, 88.84)% gait cycle
A-Ctl	8.81 [5.93, 11.68]*** (46.85, 97.53)% gait cycle	– 6.94 [– 9.55, – 4.34]* (68.17, 83.28)% gait cycle	8.77 [6.01, 11.53]*** (38.84, 90.04)% gait cycle
B-C	–	–	–
B-Ctl	4.31 [2.44, 6.18]** (70.57, 92.51)% gait cycle	–	–
C-Ctl	–	–	–

Post hoc analyses were conducted using SPM two-tailed t-tests with Bonferroni correction, solely for motions during the pre-swing and swing phases. Mean difference, 95% confidence interval, and % gait cycle used for post hoc analysis described in the table

Statistical significance denoted by * ($p < 0.05$), ** ($p < 0.01$), *** ($p < 0.001$)

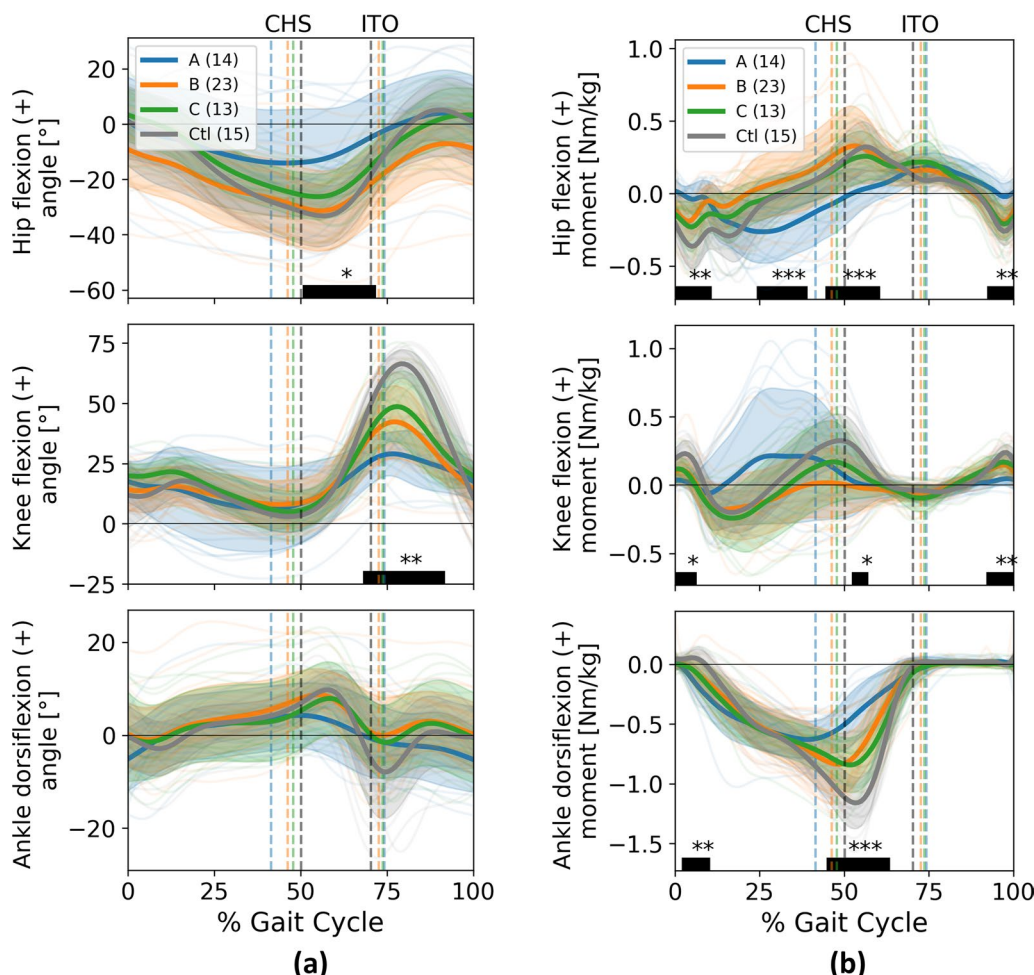


Fig. 4 The between-group comparisons of sagittal plane joint kinematics (a) and kinetics (b). The left column represents sagittal plane kinematics, and the right column represents sagittal plane kinetics. Statistics derived from SPM One-way ANOVA. Thin solid lines in backgrounds represent individual data. Left and right vertical dashed lines indicate contralateral heel strike (CHS) and ipsilateral toe-off (ITO) events, respectively. The gait cycle is based on the paretic limb's heel strike (0%)

Table 3 Summary of post hoc between-group comparisons for sagittal plane joint kinematics

Comparison	Paretic Hip Flex/Ext Angle [°]	Paretic Knee Flex/Ext Angle [°]
A-B	18.65 [7.59, 29.71]* (55.91, 69.82)% gait cycle	–
A-C	–	–18.41 [–27.70, –9.11]* (73.41, 79.86)% gait cycle
A-Ctl	20.25 [9.25, 31.26]* (54.98, 67.45)% gait cycle	–29.31 [–35.26, –23.36]*** (66.40, 91.18)% gait cycle
B-C	–	–
B-Ctl	–	–21.60 [–27.96, –15.25]*** (71.31, 92.00)% gait cycle
C-Ctl	–	–17.62 [–26.94, –8.30]* (75.13, 84.25)% gait cycle

Post hoc analyses were conducted using SPM two-tailed t-tests with Bonferroni correction, solely for motions during the pre-swing and the initial swing phases. Mean difference, 95% confidence interval, and %gait cycle used for post hoc analysis described in the table

Statistical significance denoted by * ($p < 0.05$), ** ($p < 0.01$), and *** ($p < 0.001$)

types according to clusters, which matched previously reported patterns [7, 8, 23], are described in Fig. 7. In addition to the number of modules, we examined their composition (Figure S1) and the dynamic motor control index (DMCI) Table S1. We did not observe any differences between clusters (Linear Mixed Model, $p > 0.05$) in module number, module composition, or DMCI.

Subset analysis based on clinically diagnosed SKG

We hypothesized that differences between clusters would be highlighted when we separated the participants diagnosed with SKG from the others. We performed the same analyses with all outcome measures on this subset. Figures S2–S6 summarize the findings. We did not observe

any significant differences between this subset and the overall group of stroke participants; however, significant differences were found when compared to the healthy control group.

Discussion

People with post-stroke SKG vary in etiologies and adaptations to their disabilities. Our goal was to determine out of a cohort of 50 post-stroke individuals whether there were different subtypes of SKG. We hypothesized that kinematics, kinetics, and muscle activity data would reveal these subtypes through time series cluster analysis, focusing on typical frontal plane compensatory motions. This contrasts with previous cluster studies, which primarily concentrated on sagittal plane musculature [7, 8, 23] or sagittal plane kinematics [42]. We found two of three clusters contained a higher proportion of people diagnosed with SKG, and these clusters showed differences in kinematics and kinetics from each other. However, both EMG time course analysis of muscle activity and module analyses with non-negative matrix factorization did not support the hypothesis that there were different coordination patterns between clusters. Thus, our evidence does not refute the simplest explanation that kinematic differences between clusters may represent variations in muscle coordination patterns, but are more likely related to impairment severity, as indicated by distinct propulsion asymmetry and gait speed.

Of our cohort of 50 post-stroke individuals, we found three different clusters characterized by differences in knee flexion angle, compensatory motions, and impairment level. We separated clusters using time-series data of the frontal plane compensatory motions (i.e., the compensation to SKG), rather than knee flexion kinematics to avoid bias towards that parameter. We found that despite

Table 4 Summary of post hoc between-group comparisons for the sagittal plane joint kinetics

Comparison	Paretic Hip Flex/Ext Moment [Nm/kg]	Paretic Knee Flex/Ext Moment [Nm/kg]	Paretic Ankle Dorsi/Plantar Flex Moment [Nm/kg]
A-B	–28.60 [–41.52, –15.68]*** (22.03, 58.10)% gait cycle	–	–
A-C	–	–	–
A-Ctl	–22.62 [–32.19, –13.05]*** (52.44, 63.41)% gait cycle	–	47.94 [34.37, 61.51]*** (43.59, 62.88)% gait cycle
B-C	–	–	–
B-Ctl	–	–22.46 [–32.12, –12.81]*** (48.31, 58.18)% gait cycle	36.08 [22.58, 49.59]*** (53.29, 62.12)% gait cycle
C-Ctl	–	–	–

Post hoc analyses were conducted using SPM two-tailed t-tests with Bonferroni correction, solely for motions during the pre-swing and the initial swing phases. Mean difference, 95% confidence interval, and %gait cycle used for post hoc analysis described in the table

Statistical significance denoted by * ($p < 0.05$), ** ($p < 0.01$), and *** ($p < 0.001$)

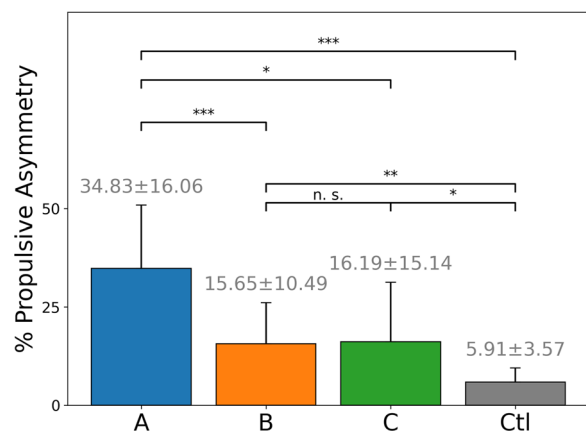


Fig. 5 Post hoc between-group comparisons for propulsive asymmetry by pairwise t-test with Bonferroni correction. Statistical significance denoted by *** ($p < 0.001$), ** ($p < 0.01$), * ($p < 0.05$), and n.s. (not significant)

excluding knee flexion angle in the clustering algorithm, the clusters could still clearly discriminate knee flexion angle and gait speed from each other. This result suggests that frontal plane motions can be used to distinguish between classes of post-stroke SKG, which are associated with functional ability. While our study did not include clinical outcome measures based on kinematic clusters as seen in a recent study [42], we did observe significant differences in paretic limb propulsion and gait speed, both of which are related to functional ability [36, 43].

Cluster A exhibited the highest level of impairment with low gait speed and high propulsion asymmetry. People in this cluster walked with greater pelvic obliquity (hip hiking), stance-phase co-contraction of the muscles around the knee, and very low knee flexion angle. Earlier work classified post-stroke gait based on muscle activation patterns. For instance, based on lower extremity EMG profiles, Knutsson and Richards found three types of disturbed motor control in post-stroke gait: Type I (premature activation of the calf muscles in early and mid-stance), Type II (no or weak activity in two or more muscles), and Type III (coactivation of major muscle groups) [44]. Shiavi and colleagues further classified Type III gait into two subgroups: one with quadriceps and hamstring coactivation during stance (Type III-S) and the other during the transition periods (Type III-T) [45]. Inappropriate stance-phase hamstrings activation of the affected side, observed in Cluster A, was similar to Type III-S. It has been suggested that Type III-S gait is compensating for a diminished ankle plantarflexor moment with stance phase hip extensor moment or forward postural lean [46]. Prolonged activity of the hamstrings and coactivation around the knee joint could be considered as a merged muscle coordination pattern from hip abductors, hip/knee extensors and hamstrings [8, 23, 47], which is denoted as MS2 in Fig. 7. Indeed, our data is consistent with this hypothesis, showing excessive hip extensor moment during stance in Cluster A (Fig. 4 and Table 4). Additionally, early pre-swing initiation of pelvic

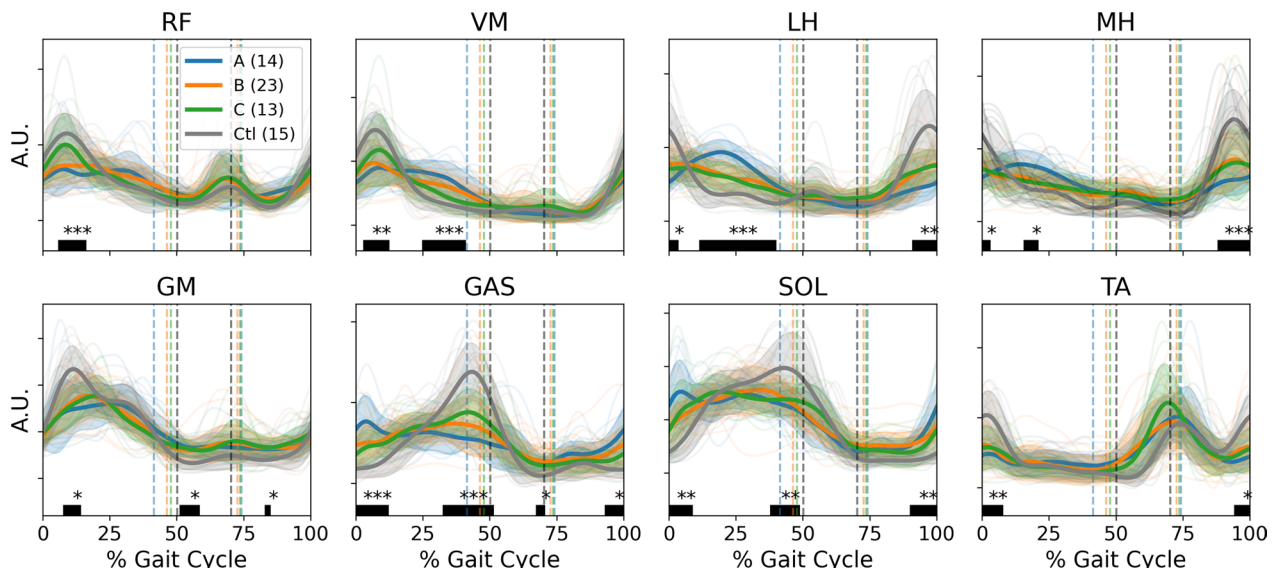


Fig. 6 Cluster-based SPM One-way ANOVA of EMG activity. RF: rectus femoris; VA: vastus medialis; LH: lateral hamstrings; MH: medial hamstrings; GM: gluteus medius; GAS: medial gastrocnemius; SOL: soleus; TA: tibialis anterior. Thin solid lines in backgrounds represent individual data. Left and right vertical dashed lines indicate contralateral heel strike (CHS) and ipsilateral toe-off (ITO) events, respectively. The gait cycle is based on the paretic limb's heel strike (0%)

Table 5 Summary of post hoc between-group comparisons of EMG activity

Comparison	Paretic Vastus medialis EMG [A.U.]	Paretic Lateral hamstrings EMG [A.U.]
A-B	–	0.59 [0.36, 0.82]*** (16.10, 28.18)% gait cycle
A-C	–	0.62 [0.36, 0.89]*** (16.32, 29.17)% gait cycle
A-Ctl	0.78 [0.50, 1.05]*** (23.44, 40.34)% gait cycle	0.89 [0.69, 1.09]*** (11.30, 40.63)% gait cycle
B-C	–	–
B-Ctl	0.53 [0.32, 0.74]*** (27.89, 42.51)% gait cycle	0.56 [0.32, 0.81]** (13.29, 22.81)% gait cycle 0.45 [0.28, 0.62]** (31.13, 40.03)% gait cycle
C-Ctl	–	–

Post hoc analyses were conducted using SPM two-tailed t-tests with Bonferroni correction. Mean difference, 95% confidence interval, and % gait cycle used for post hoc analysis described in the table

Statistical significance denoted by * ($p < 0.05$), ** ($p < 0.01$), and *** ($p < 0.001$)

obliquity is often used to improve balance [46]. This early hip hiking characterizes Cluster A. Cluster A was primarily composed of those diagnosed with SKG (10 out of 14). They were the most impaired, as evidenced by the lowest gait speed, knee flexion, modules, and the highest propulsion asymmetry. Cluster B, on the other hand, exhibited greater gait speed and better propulsion asymmetry than Cluster A. People in this group walked with large hip hiking and hip abduction motions in swing, excessive quadriceps activation during stance, and reduced swing knee flexion angle compared to healthy controls. The characteristics of this cluster were similar to the previously reported combination of modules, denoted as MS1 in Fig. 7. This combined pattern was characterized by opposing functions, such as prolonged braking and

early propulsion, resulting in an altered paretic leg swing. Excessive quadriceps activity during stance, coupled with soleus and gastrocnemius activation, would cause insufficient foot clearance, leading to a combination of hip hiking and hip abduction [8]. Fujita and colleagues recently reported the muscle module characteristics in post-stroke individuals. They identified the same altered muscle modules, MS1 and MS2, observed in this study, within their post-stroke SKG group [26].

Cluster B may be associated with quadriceps spasticity, or more specifically, hyperreflexia. Our previous work observed hip abduction in a small cohort diagnosed with SKG and applied robotic knee flexion perturbations during walking [18]. We found that assistance increased hip abduction instead of the hypothesized drop of the supposed compensatory motion. Our later analysis revealed that the robotic assistance likely evoked a spastic quadriceps response, and this response was coupled with hip abductor activation [19]. In a new group of post-stroke SKG individuals, we found that quadriceps reflex excitability was highly correlated to knee flexion kinematics [9]. Even though there were similar levels of knee flexion between those post-stroke and healthy individuals, only post-stroke individuals exhibited excessive hip abduction, suggesting a neural basis for an ostensible compensation. Further work would need to be conducted to conclude whether Cluster B is reflective of this phenomenon and correlated with quadriceps hyperreflexia.

People in Cluster C had reduced propulsion and hamstrings activity compared to healthy controls, but knee flexion and all other parameters were closest to healthy controls of the clusters. While Clusters A and B contained the majority of those diagnosed with SKG, Cluster C still contained 3 out of 14. Since individuals in Cluster C had the highest knee flexion angle, it is not surprising that they were clustered with the lowest amount of

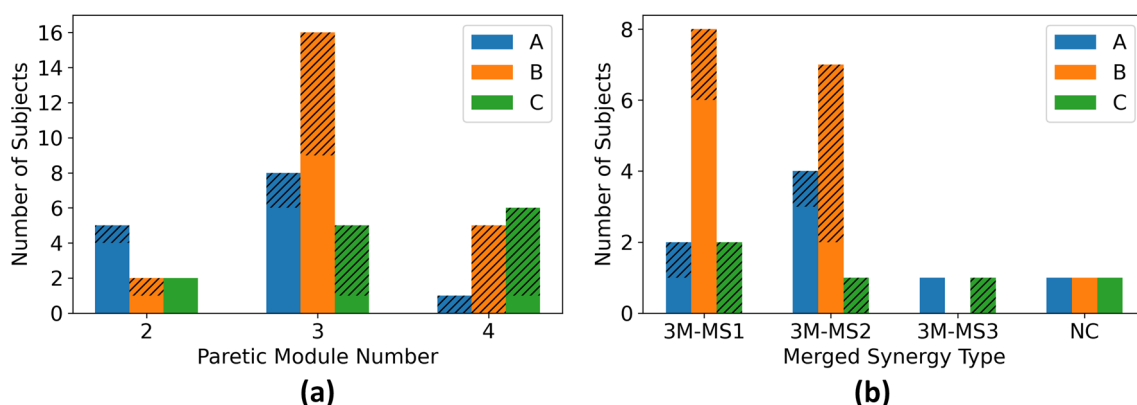


Fig. 7 Breakdown of number of muscle modules per post-stroke participant (a) and merged synergy type in those with three modules (b). Cross-hatched portions indicate non-SKG participants

frontal plane compensatory motions. The definition of SKG is vague, but literature is converging towards knee flexion angle below 45° [48, 49], which encompasses a large range of people with post-stroke gait impairments. Our recommendation is to have more specific, functionally relevant definitions of SKG to obtain better consistency between studies.

One of the most interesting results is the lack of observed differences in muscle coordination patterns between clusters. We expected that individuals with measurably different walking patterns would exhibit distinct muscle coordination patterns. However, our analysis did not reveal strong statistical significance in the differences in muscle coordination patterns between clusters. We interpret this null finding to three non-exclusive possibilities: first, that while we recorded from 8 different major muscles, primarily in the sagittal plane, we might have observed coordination differences if other muscles were recorded, particularly trunk muscles responsible for pelvic obliquity. Second, it may be that the lack of observed difference in coordination patterns between clusters means that the differences between SKG-based clusters are based on differences in dynamics necessitated by the severity of impairment rather than a different coordination pattern. Third, we may not have examined a sufficient sample size to detect significant differences between the clusters.

The findings from this study have no bearing on the causes of SKG, but rather the characterization. Certain limitations need to be considered when interpreting the results. For example, although we examined 50 participants this number may still be insufficient to generalize the findings to the entire population of people with stroke. Circumduction was based on joint angles rather than lateral foot displacement [50], which could result in slightly different observations compared to other contemporary studies. We also relied on a single clinical expert rather than a group of experts. Although the SKG diagnosis might have differed with multiple experts, the absence of a true gold standard suggests that these variations in diagnosis may not be substantial.

The novelty of this work lies in two aspects: (1) the use of time-series cluster analysis to identify distinct subtypes of individuals with post-stroke SKG without losing critical information, and (2) the classification of these subtypes based on the effects of SKG, compensatory movements resulting from reduced knee flexion. Classifying and characterizing these subtypes may help improve treatment approaches, standardize research methodologies, and uncover the reasons behind treatment non-responsiveness, ultimately leading to more effective and personalized healthcare solutions. Furthermore, incorporating advanced computer

vision-based motion analysis techniques in future research could enable our clustering framework to serve as a foundation for developing more accessible diagnostic tools beyond traditional gait biomechanics laboratory settings.

Conclusion

In this study, we examined kinematics, kinetics and muscle activity of 50 post-stroke individuals, some of whom were clinically diagnosed with SKG. Since SKG may arise from different causes and people may compensate for the disability in multiple ways, we hypothesized that there are different subtypes of SKG. Our time-series cluster analysis based on gait compensations resulted in 3 clusters, 2 of which could be considered different subtypes: one type, with the slowest gait speed, relying mostly on pelvic obliquity, and another type, with faster gait speed, using a combination of pelvic obliquity and hip abduction. The subtypes are consistent with gait patterns found in previous work. We hypothesized that these groups would show differences in underlying motor coordination, but our evidence does not support this finding. The differences between clusters would be most likely due to different levels of gait impairment. We recommend more specific definitions of post-stroke SKG and more work to determine differences in underlying causes, rather than being a different type of SKG.

Supplementary Information

The online version contains supplementary material available at <https://doi.org/10.1186/s12984-025-01582-3>.

Supplementary Material 1.

Author contributions

As the primary author, JL managed the data processing/analysis, interpretation of results, preparation of figures and tables, and main manuscript writing. BAS assisted with data processing/analysis and interpretation of results. RKL provided the clinical diagnoses. JS, SAK, and RAN guided the study's conceptualization and contributed to interpreting the findings. All authors reviewed and approved the final manuscript.

Funding

This work was supported by the NICHD under the National Institutes of Health under the Award Number R01HD100416. The contents are solely the responsibility of the authors and do not necessarily represent the official views of the NIH or NICHD. The funders had no role in study design, data collection and analysis, decision to publish, or preparation of the manuscript. Partial funding for this project was provided by the VA Office of Research and Development (ORD), with additional support from the VA/ORD Rehabilitation R&D Service (1IK6 RX003075) and the National Institutes of Health (NIH P20 GM109040). The contents are solely the responsibility of the authors and do not necessarily represent the official views of the VA, NIH or NICHD. The funders had no role in study design, data collection and analysis, decision to publish, or preparation of the manuscript.

Availability of data and materials

The data used in this study are available from the Center of Biomedical Research Excellence in Stroke Recovery upon reasonable request.

Declarations

Ethics approval and consent to participate

This analysis used deidentified retrospective data from a research database maintained by the NIH-funded Center of Biomedical Research Excellence in Stroke Recovery (NIH P20 GM109040). The research database is approved by the Medical University of South Carolina's Institutional Review Board in accordance with the Declaration of Helsinki. All participants signed an informed consent prior to study enrollment agreeing to have their data archived for future research.

Consent for publication

I understand that the information will be published without my/my child or ward's/my relative's (circle as appropriate) name attached, but that full anonymity cannot be guaranteed. I understand that the text and any pictures or videos published in the article will be freely available on the internet and may be seen by the general public. The pictures, videos and text may also appear on other websites or in print, may be translated into other languages or used for commercial purposes. I have been offered the opportunity to read the manuscript.

Competing interests

The authors declare no competing interests.

Received: 6 October 2024 Accepted: 17 February 2025

Published online: 25 February 2025

References

- Merlo A, Campanini I. Impact of instrumental analysis of stiff knee gait on treatment appropriateness and associated costs in stroke patients. *Gait Posture*. 2019;72:195–201.
- Chantry F, Schreiber C, Pereira JAC, Kaps J, Dierck F. Classification of Stiff-Knee gait kinematic severity after stroke using retrospective k-means clustering algorithm. *J Clin Med*. 2022;11:6270.
- Perry J, Burnfield JM. Gait analysis: normal and pathological function. *J Sports Sci Med*. 2010;9:353.
- Tenniglo MJB, et al. Influence of functional electrical stimulation of the hamstrings on knee kinematics in stroke survivors walking with stiff knee gait. *J Rehabil Med*. 2018;50:719–24.
- Li S. Stiff Knee gait disorders as neuromechanical consequences of spastic hemiplegia in chronic stroke. *Toxins*. 2023;15:204.
- Campanini I, Merlo A, Damiano B. A method to differentiate the causes of Stiff-Knee gait in stroke patients. *Gait Posture*. 2013;38:165–9.
- Clark DJ, Ting LH, Zajac FE, Neptune RR, Kautz SA. Merging of healthy motor modules predicts reduced locomotor performance and muscle coordination complexity post-stroke. *J Neurophysiol*. 2010;103:844–57.
- Van Criekinge T, et al. Lower limb muscle synergies during walking after stroke: a systematic review. *Disabil Rehabil*. 2020;42:2836–45.
- Akbas T, et al. Rectus femoris hyperreflexia contributes to Stiff-Knee gait after stroke. *J NeuroEngineering Rehabil*. 2020;17:117.
- Tenniglo MJ, et al. Effect of chemodenervation of the rectus femoris muscle in adults with a stiff knee gait due to spastic paresis: a systematic review with a meta-analysis in patients with stroke. *Arch Phys Med Rehabil*. 2014;95:576–87.
- Tenniglo MJB, Nene AV, Rietman JS, Buurke JH, Prinsen EC. The effect of botulinum toxin type A injection in the rectus femoris in stroke patients walking with a stiff knee gait: a randomized controlled trial. *Neurorehabil Neural Repair*. 2023;37:640–51.
- Sutherland DH, Santi M, Abel MF. Treatment of Stiff-Knee gait in cerebral palsy: a comparison by gait analysis of distal rectus femoris transfer versus proximal rectus release. *J Pediatr Orthop*. 1990;10:433.
- De Quervain IAK, Simon SR, Leurgans S, Pease WS, McAllister D. Gait pattern in the early recovery period after stroke. *JBJS*. 1996;78:1506.
- Piazza SJ, Delp SL. The influence of muscles on knee flexion during the swing phase of gait. *J Biomech*. 1996;29:723–33.
- Sutherland DH, Davids JR. Common gait abnormalities of the knee in cerebral palsy. *Clin Orthop Relat Res*. 1993;288(139):1976–2007.
- Kerrigan DC, Frates EP, Rogan S, Riley PO. Hip hiking and circumduction: quantitative definitions. *Am J Phys Med Rehabil*. 2000;79:247–52.
- Stanhope VA, Knarr BA, Reisman DS, Higginson JS. Frontal plane compensatory strategies associated with self-selected walking speed in individuals post-stroke. *Clin Biomech*. 2014;29:518–22.
- Sulzer JS, Gordon KE, Dhaher YY, Peshkin MA, Patton JL. Preswing knee flexion assistance is coupled with hip abduction in people with Stiff-Knee gait after stroke. *Stroke*. 2010;41:1709–14.
- Akbas T, et al. Hip circumduction is not a compensation for reduced knee flexion angle during gait. *J Biomech*. 2019;87:150–6.
- Allen JL, Kautz SA, Neptune RR. The influence of merged muscle excitation modules on post-stroke hemiparetic walking performance. *Clin Biomech*. 2013;28:697–704.
- Ting LH, et al. Neuromechanical principles underlying movement modularity and their implications for rehabilitation. *Neuron*. 2015;86:38–54.
- Brough LG, Kautz SA, Bowden MG, Gregory CM, Neptune RR. Merged plantarflexor muscle activity is predictive of poor walking performance in post-stroke hemiparetic subjects. *J Biomech*. 2019;82:361–7.
- Mizuta N, et al. Merged swing-muscle synergies and their relation to walking characteristics in subacute post-stroke patients: an observational study. *PLoS ONE*. 2022;17:e0263613.
- Lewek MD, Hornby TG, Dhaher YY, Schmit BD. Prolonged quadriceps activity following imposed hip extension: a neurophysiological mechanism for Stiff-Knee gait? *J Neurophysiol*. 2007;98:3153–62.
- Akbas T, Neptune RR, Sulzer J. Neuromusculoskeletal simulation reveals abnormal rectus femoris-gluteus medius coupling in post-stroke gait. *Front Neurol*. 2019;10:301.
- Fujita K, et al. Altered muscle synergy structure in patients with post-stroke stiff knee gait. *Sci Rep*. 2024;14:20295.
- Burden A. How should we normalize electromyograms obtained from healthy participants? What we have learned from over 25 years of research. *J Electromyogr Kinesiol*. 2010;20:1023–35.
- Delp SL, et al. OpenSim: open-source software to create and analyze dynamic simulations of movement. *IEEE Trans Biomed Eng*. 2007;54:1940–50.
- Phinyomark A, Petri G, Ibáñez-Marcelo E, Osis ST, Ferber R. Analysis of big data in gait biomechanics: current trends and future directions. *J Med Biol Eng*. 2018;38:244–60.
- Pataky TC. Generalized n -dimensional biomechanical field analysis using statistical parametric mapping. *J Biomech*. 2010;43:1976–82.
- Dhillon IS, Guan Y, Kulik B. Kernel k-means: spectral clustering and normalized cuts. In: Proceedings of the tenth ACM SIGKDD international conference on Knowledge discovery and data mining. New York: Association for Computing Machinery; 2004. pp. 551–556. <https://doi.org/10.1145/1014052.1014118>.
- Cuturi M. Fast global alignment kernels. In: Proceedings of the 28th international conference on machine learning (ICML-11). 2011. pp. 929–36.
- Tavenard R, et al. Tslearn, a machine learning toolkit for time series data. *J Mach Learn Res*. 2020;21:1–6.
- Rousseeuw PJ. Silhouettes: a graphical aid to the interpretation and validation of cluster analysis. *J Comput Appl Math*. 1987;20:53–65.
- Kodinariya TM, Makwana PR. Review on determining number of cluster in K-means clustering. *Int J*. 2013;1:90–5.
- Roelker SA, Bowden MG, Kautz SA, Neptune RR. Paretic propulsion as a measure of walking performance and functional motor recovery post-stroke: a review. *Gait Posture*. 2019;68:6–14.
- Steele KM, Rozumalski A, Schwartz MH. Muscle synergies and complexity of neuromuscular control during gait in cerebral palsy. *Dev Med Child Neurol*. 2015;57:1176–82.
- Collimore AN, Aiello AJ, Pohlig RT, Awad LN. The dynamic motor control index as a marker of age-related neuromuscular impairment. *Front Aging Neurosci*. 2021;13:678525.
- Pataky TC. One-dimensional statistical parametric mapping in Python. *Comput Methods Biomed Eng*. 2012;15:295–301.
- Seabold S, Perktold J, Statsmodels: econometric and statistical modeling with python. *SciPy*. 2010;7:1.

41. Neptune RR, Clark DJ, Kautz SA. Modular control of human walking: a simulation study. *J Biomech.* 2009;42:1282–7.
42. Mizuta N, et al. Characteristics of limb kinematics in the gait disorders of post-stroke patients. *Sci Rep.* 2024;14:3082.
43. Awad LN, Lewek MD, Kesar TM, Franz JR, Bowden MG. These legs were made for propulsion: advancing the diagnosis and treatment of post-stroke propulsion deficits. *J NeuroEng Rehabil.* 2020;17:139.
44. Knutsson E, Richards C. Different types of disturbed motor control in gait of hemiparetic patients. *Brain.* 1979;102:405–30.
45. Richard Shiavi PD, Bugle HJ, Limbird T. Electromyographic gait assessment, Part 2: preliminary assessment of hemiparetic synergy patterns. *J Rehabil Res.* 1987;24:24–30.
46. Olney SJ, Richards C. Hemiparetic gait following stroke. Part I: characteristics. *Gait Posture.* 1996;4:136–48.
47. Souissi H, Zory R, Bredin J, Roche N, Gerus P. Co-contraction around the knee and the ankle joints during post-stroke gait. *Eur J Phys Rehabil Med.* 2018;54:380–7.
48. Kerrigan DC, Gronley J, Perry J. Stiff-legged gait in spastic paresis a study of quadriceps and hamstrings muscle activity. *Am J Phys Med Rehabil.* 1991;70:294.
49. Lee J, et al. Between-limb difference in peak knee flexion angle can identify persons post-stroke with Stiff-Knee gait. *Clinical Biomechanics.* 2024;120:106351. <https://doi.org/10.1016/j.clinbiomech.2024.106351>
50. Shorter KA, Wu A, Kuo AD. The high cost of swing leg circumduction during human walking. *Gait Posture.* 2017;54:265–70.

Publisher's Note

Springer Nature remains neutral with regard to jurisdictional claims in published maps and institutional affiliations.